ORGANOMETALLICS

Article

pubs.acs.org/Organometallics

Ferrocene–Biotin Conjugates Targeting Cancer Cells: Synthesis, Interaction with Avidin, Cytotoxic Properties and the Crystal Structure of the Complex of Avidin with a Biotin–Linker–Ferrocene Conjugate

Damian Plażuk,[†] Janusz Zakrzewski,*[,†] Michèle Salmain,[‡] Andrzej Błauż,[§] Błażej Rychlik,[§] Paweł Strzelczyk,[∥] Anna Bujacz,[∥] and Grzegorz Bujacz[∥]

[†]Department of Organic Chemistry, Faculty of Chemistry, University of Łódź, Tamka 12, 91-403 Łódź, Poland

[‡]Chimie ParisTech, Laboratoire Charles Friedel, and CNRS, UMR 7223, 11 rue Pierre et Marie Curie, F-75005 Paris, France

[§]Cytometry Laboratory, Department of Molecular Biophysics, Faculty of Biology and Environmental Protection, University of Łódź, 12/16 Banacha Street, 90-237 Łódź, Poland

[∥]Institute of Technical Biochemistry, Łódź University of Technology, Stefanowskiego 4/10, 90-924 Łódź, Poland

Supporting Information

ABSTRACT: Friedel–Crafts acylation of ferrocene with a biotin-derived carboxylic acid having 6-aminohexanoyl linkers attached to the biotin carboxylic group and with desthiobiotin afforded the corresponding ferrocene–biotin bioconjugates. These compounds as well as biotinyl ferrocenyl ketone exhibit high affinity for avidin. Their cytotoxicity against cancer cell lines having various levels of biotin receptors (SMVT) was measured and revealed that lines displaying high levels of SMVT (SW620) were the most susceptible. This suggests that biotin serves as a biological vector delivering cytotoxic ferrocenyl moieties to cancer cells. The crystal structure of the complex of avidin with a conjugate having two linker units between biotin and ferrocene was determined and revealed stabilization of several different conformations of the ligand within the protein binding pocket.

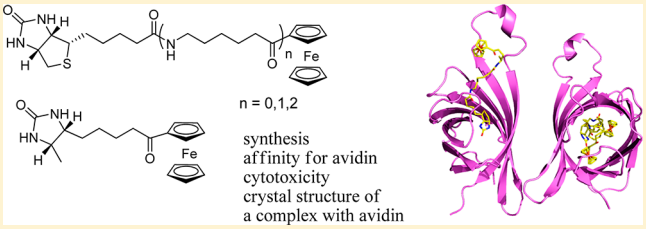

INTRODUCTION

The bioorganometallic chemistry of ferrocene continues to attract significant interest mainly due to the anticancer activity of numerous ferrocene derivatives.[1] Pioneering work in this field was done by Jaouen and his co-workers, who demonstrated that diverse ferrocenyl compounds structurally related to a classical antibreast cancer drug, tamoxifen, exhibited a broad spectrum of cytotoxic activity, with IC_{50} values in some cases being in the submicromolar range.[2] Another promising and intensively developed axis of research in this field deals with ferrocenyl compounds exhibiting antimalarial activity.[3]

We recently disclosed the synthesis of a novel type of ferrocene–biotin conjugate, biotinyl ferrocenyl ketone **1**, via direct Friedel–Crafts acylation of ferrocene with biotin (Scheme 1).[4] We expected that ferrocenyl–biotin conjugates might exhibit enhanced anticancer activity—it is well established that biotin (vitamin H) is necessary for cell growth and many rapidly growing cancer cells have high levels of a specific vitamin receptor (sodium-dependent multivitamin transporter, SMVT) on their surface.[5] Therefore, biotin may serve as a biological vector for the selective delivery of cytotoxic compounds to the cancer cells.[6] In this paper we demonstrate the applicability of this approach in the design of anticancer ferrocenyl compounds. From this standpoint it was interesting to compare the cytotoxic activity of **1** with that of analogues having the bicyclic biotin and the ferrocenyl moieties separated

Scheme 1. Synthesis of Biotin–Ferrocene Conjugates 1–4

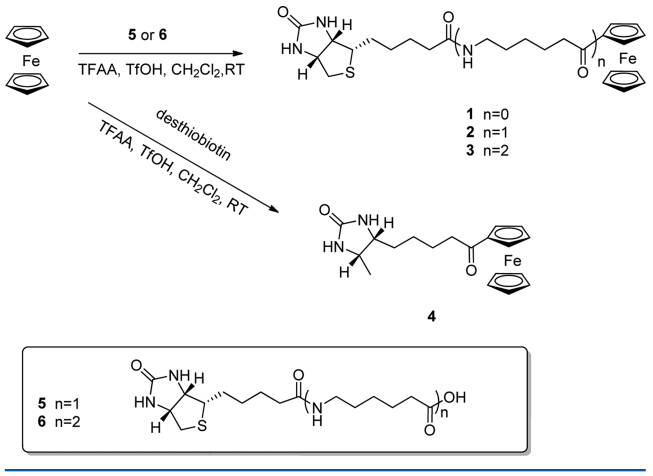

Special Issue: Ferrocene - Beauty and Function

Received: April 11, 2013

   dx.doi.org/10.1021/om4003126 | *Organometallics* XXXX, XXX, XXX–XXX

Scheme 2. Acylation of Ferrocene with 6-Acetamidohexanoic Acid (7)

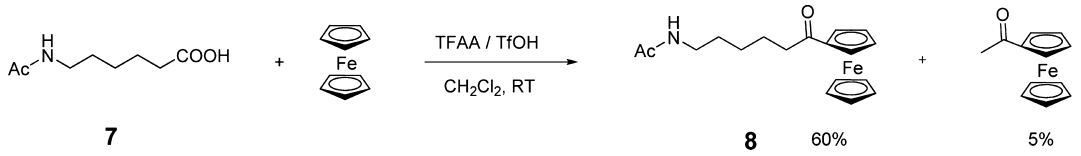

7 8 60% 5%

by longer spacer arms. Furthermore, we intended to compare the cytotoxic activity of **1** with that of its desthiobiotinyl analogue, which is expected to have a lower affinity for the target receptor (as evidenced for avidin).[7] For this purpose we synthesized analogues of **1** featuring one and two 6-aminohexanoic spacers between the biotin fragment and ferrocene (**2** and **3**, respectively) and the desthiobiotin conjugate **4**. We measured the affinity of **1**–**4** for avidin and studied their cytotoxic properties against selected cancer cells expressing different levels of SMVT. Finally, to gain insight into the interaction of biotinylated ferrocenes with avidin, we solved the X-ray structure of the complex of avidin with compound **3**.

RESULTS AND DISCUSSION

Synthesis of 2–4. The synthesis of **1** was reported in our earlier work.[4] This compound was formed in 55% yield from the Friedel–Crafts reaction of ferrocene with biotin in the presence of trifluoroacetic anhydride (TFAA) and trifluoromethanesulfonic (triflic) acid (TfOH). Ruthenocene, pyrene,[4] and several other arenes[8] react similarly. Compounds obtained in this way constitute a novel class of biotin derivatives, having a C–C bond linking the carbonyl group in the biotin valeryl chain with a biotinylated moiety. Their advantage over the more common biotin conjugates having amide bonds between biotin and the biotinylated entity is improved resistance to biotinidase,[9] an enzyme present in biological samples that cleaves the C–N bond in biotin amides.

In a continuation of our research program, which is focused on the use of functionalized and biologically relevant acids in Friedel–Crafts-type reactions,[4,10] we became interested in the possibility of synthesis of biotin–ferrocene conjugates having aliphatic 6-aminohexanoic linkers between the biotin and ferrocene entities directly from acids **5** and **6** and ferrocene. Since we were aware of the instability of the amide bond and the acylating ability of amides in strongly acidic media used in Friedel–Crafts reactions,[11] we decided to start by studying the reaction of ferrocene with 6-acetamidohexanoic acid (**7**), chosen as a model acid containing an amide bond, similar to those present in **5** and **6**. We found that this reaction, performed in the presence of TFAA and TfOH in dichloromethane at room temperature, afforded ketone **8** in a satisfactory yield (60%) along with a small amount (5%) of acetylferrocene (Scheme 2).

In the literature there are only a few reports on the use of acid derivatives containing amide groups as arene acylating reagents.[12] They are all limited to some *N*-acylated α-amino acid chlorides or esters. β-Amidoacylation of ferrocene was achieved using strained *N*-acylated azetidinones in a superacidic medium in a reaction involving cleavage of the C(=O)–N bond in the acylating agent.[13] Therefore, the synthesis of **8** provides evidence that a carboxylic acid containing a remote amide functionality may be used, under the appropriate experimental conditions, as an efficient acylating reagent in a Friedel–Crafts reaction. The formation of acetylferrocene reveals a weak acylating ability of the acetamido moiety present in **7** and is in line with recent work disclosing triflic acid promoted Friedel–Crafts-type reactions with amides and ureas.[11]

Encouraged by these results, we performed the reaction of ferrocene with acids **5** and **6** under the same conditions. We isolated the expected biotinylated ferrocenes **2** and **3**, albeit in significantly lower yields (28% and 16%, respectively). This result shows that, in principle, acids containing 6-aminohexanoic linkers may be used as acylating agents in Friedel–Crafts reactions, but in this case the acid/TFAA/TfOH system works less efficiently. Fortunately, the isolation procedure for **2** and **3** is relatively easy (see the Experimental Section). Finally, the reaction of ferrocene with desthiobiotin afforded compound **4** in a 34% yield (Scheme 1).

Interactions of 1–4 with Avidin. *Relative Binding Affinity of 1–4 to Avidin.* The association of avidin with biotin and its derivatives has attracted a great amount of interest because of the exceptional strength of these species ($K_a \approx 10^{15}$ M^{-1} for the parent biotin) and the wide range of applications.[14] In a previous paper[4] we had applied a solid-phase competitive enzymatic assay to determine the relative binding affinity (RBA) of **1** to avidin and its ruthenocenyl and pyrenyl analogues. In this paper we applied this method to determine the IC_{50}'s together with the RBA's of complexes **2**–**4**. The results are shown in Table 1.

Table 1. Values of IC_{50} and the Relative Binding Affinities (RBA's) of Biotin, Desthiobiotin, and Conjugates 2–4 for Avidin

compd	IC_{50} (nM)	RBA (%)
biotin	9.0 ± 2.1	100
1	33 ± 2.0	73[a]
2	20.3 ± 1.8	44 ± 4
3	18 ± 2.0	50 ± 5
desthiobiotin	21.6 ± 6.5	42 ± 10
4	25.4 ± 4.8	35 ± 5

[a]Reference 4. IC_{50}(biotin) = 24 ± 7 nM.

The RBA of **1** was found to be equal to 73% in our earlier work.[4] This means that the introduction of one or two 6-aminohexanoic acid linkers did not increase the affinity of bioconjugates **2** and **3** for avidin, although a conjugate with a longer linker (**3**) has a slightly higher affinity than **2**. As reported in the literature,[7] the affinity of desthiobiotin for avidin is significantly lower than that of biotin. Interestingly, in this case appending a ferrocenyl substituent practically did not influence the RBA value.

Cytotoxicity of Ferrocene Conjugates. Biotin is a growth promoter at the cellular level, and its content in tumors is substantially higher than that in normal tissues. As mammals are not able to biosynthesize biotin, they utilize the two main sources of this vitamin: food and symbiotic bacteria inhabiting the colon. Biotin is taken up from the intestinal content via the sodium-dependent multivitamin transporter (SMVT),[5] a product of the *Slc5a6* gene that is expressed in the apical

dx.doi.org/10.1021/om4003126 | *Organometallics* XXXX, XXX, XXX–XXX

region of the epithelial cells. We thought that it would be interesting to study whether the biotin−ferrocene conjugates had a cytotoxic effect on cancer cell lines and also to check whether the response of these cancer cells to the biotin−ferrocene conjugates correlates with the level of SMVT (or *Slc5a6*). For this purpose, we selected three different human intestine derived tumor cell lines: COLO-205 (colon adenocarcinoma), HCT116 (colon carcinoma), and SW620 (colon adenocarcinoma).

The level of expression of the *Slc5a6* gene was determined for the three selected cell lines. *Slc5a6* mRNA was the most abundant in SW620 cells (10.4 ± 4.4 copies per 1000 copies of the reference gene, n = 3), while COLO-205 and HCT116 exhibited the same level of expression (3.6 ± 1.1 and 3.6 ± 1.8 copies per 1000 copies of the reference gene, n = 3, respectively).

The cytotoxicity of the ferrocene−biotin conjugates was tested within the range of 3 nM to 30 μM (we did not use higher concentrations, as they would be highly above a realistic assumption of concentration achievable in any compartment of a living organism). The results are gathered in Table 2 and Figure 1.

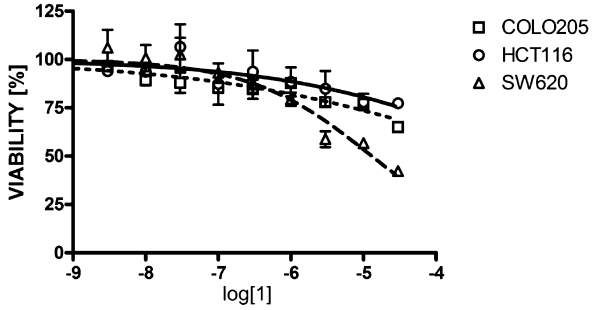

Figure 1. Viability of various tumor cell lines in the presence of biotin−ferrocenyl conjugate **1** (for compounds **2**−**4** and **8** see the Supporting Information).

As can be seen from Table 2, SW620 cells are the most susceptible to conjugates **1**, **2**, **4**, and **8**. The COLO-205 and HTT116 cells are resistant to these compounds, with one exception (HCT116 cells and compound **3**). Therefore, the correlation between the susceptibility of cells to the compounds under study and *Slc5a6* expression is clear. Conjugate **1** was the most toxic to the SW620 cells (IC_{50} = 13.0 ± 3.6 μM), being approximately twice as potent as **2** (IC_{50} = 26.2 ± 1.4 μM), which in turn was much more potent than **3**. This means that 6-aminohexanoyl spacers exert a deleterious effect on the cytotoxic activity of the investigated conjugates. The cytotoxic activity of the desthiobiotin−ferrocene conjugate **4** against the SW620 cells is approximately 6 times weaker (IC_{50} = 78.5 ± 1.9 μM) than that of **1**. It is comparable to that of compound **8** (IC_{50} = 70.1 ± 1.8 μM), which is an analogue of **2**, having an acetyl group in the place of the biotin moiety. The above data clearly confirm the crucial role of the biotin moiety in the cytotoxic activity of the compounds under study. In contrast, the presence of the desthiobiotin moiety in compound **4** did not seem to enhance its cytotoxic activity.

Table 2. Susceptibility of Colon Cancer Cells to Biotin−Ferrocene Conjugates[a]

	IC_{50} (μM)		
compd	COLO-205	HCT116	SW620
1	≫100	NA	13.0 ± 3.6
2	≫100	NA	26.2 ± 1.4
3	≫100	87.5 ± 1.8	≫100
4	≫100	≫100	78.5 ± 1.9
8	≫100	NA	70.1 ± 1.8

[a] IC_{50} values are given in μM. NA denotes that the data did not allow calculation of the IC_{50} parameter. Values given as ≫100 denote that the calculated IC_{50} parameter value is highly above 100 μM.

The idea of using biotin as a vector to deliver a cytotoxic agent to cancer cells overexpressing biotin receptors (SMVT) was applied earlier by Ojima[6] to improve the cytotoxic properties of taxoids. In this context, it should be emphasized that many cancer cells overexpress biotin receptors more than they do folate and/or vitamin B_{12} receptors, which until now were more widely used as biomarkers in targeted chemotherapy.[5] Other reports on highly cytotoxic biotin conjugates of natural products have also appeared in the literature.[15] The results obtained in this work clearly indicate that biotin can also be used for tumor-targeted delivery of a cytotoxic ferrocene moiety. Therefore, cytotoxic biotin−ferrocene conjugates are promising candidates for anticancer drugs.

X-ray Structure of the Complex of Avidin with Compound ***3***. We attempted to obtain crystals of complexes of avidin with compounds **1**−**4** suitable for X-ray diffraction studies. However, so far we succeeded only in the case of the complex of avidin with the conjugate **3** (hereafter denoted as **avidin-3**). Crystals of this complex were obtained by the hanging drop vapor-diffusion technique. Its X-ray structure reveals interesting features related to protein−organometallic ligand interactions.

The model consists of residues 2−125 of monomer **A** and 2−124 of monomer **B**, which are quite visible on the electron density map. The overall fold of the protein and its tetrameric arrangement are similar to those described earlier.[16] Each monomer is constructed of eight antiparallel strands, which form a β-barrel with the binding site for biotin or a derivative located at its wider part (Figure 2). The monomer is stabilized by one disulfide bridge, three intermolecular salt bridges, and intramolecular hydrogen bonds.[17]

Figure 2. Crystal structure of **avidin-3**.

In the orthorhombic crystalline form, one molecular dyad is coincident with the crystallographic 2-fold axis; thus, an avidin

dx.doi.org/10.1021/om4003126 | *Organometallics* XXXX, XXX, XXX−XXX

dimer is located in the asymmetric unit. Therefore, the quaternary structure of avidin has been described as a dimer of dimers.

The tertiary and quaternary structures of **avidin-3** are generally similar to those of other biotin–avidin complexes (PDB ID: 2AVI and 1AVD).[16] However, several noteworthy differences are evident. The set of hydrogen-bond interactions is almost identical with that of the avidin–biotin complex with respect to the bicyclic ring system. The ligand is stabilized in the binding pocket through hydrogen bonds (Table 3; the atom numbering scheme is shown in Figure 3), van der Waals contacts, and hydrophobic interactions.

Table 3. Hydrogen Bond Protein–Ligand Interactions in avidin-3

	3			
	monomer **A**		monomer **B**	
avidin	atom	distance (Å)	atom	distance (Å)
Ser16 OH	O1	2.98	O1	2.86
Tyr33 OH	O1	2.88	O1	2.84
Asn12 NH_2	O1	3.12	O1	3.11
Thr35 OH	N2	2.98	O4	3.02[a]
Asn118 O	N1	2.94	N1	2.95
Thr77 OH	S1	3.01	S1	3.07
Ala39 NH	O2	2.57		
Thr38 OH	O2	2.89		
Ser75 OH	N3	3.08	O2	3.44[a]
Ser73 OH			O2	3.47[a]

[a]Conformation II of **3**.

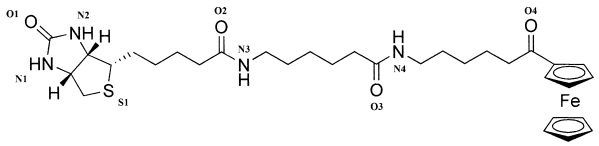

Figure 3. Polar atom numbering scheme for **3**.

The overall structure of monomer **A** differs from that of monomer **B** in the areas of loops L3-4 (residues 35–45) and L6-7 (residues 85–90) (Figure 4). As a result, in the crystal structure of **avidin-3**, ligand **3** adopts a single conformation in monomer **A**, whereas in monomer **B** the ligand adopts two different conformations (Figure 5).

In monomer **A** ligand **3** is stabilized in the binding pocket by nine direct hydrogen bonds and four van der Waals contacts. In the deepest part of the cavity several polar residues are available for hydrogen bonding to atoms of the ureido fragment. Nitrogen N1 interacts with the oxygen of Asn118, N2 interacts with the hydroxyl group of Thr35, and O1 acts as an acceptor for three donor groups: OH of Ser16, OH of Tyr33, and NH_2 of Asn12. On the other side of the pocket the sulfur atom (S1) in a tetrahydrothiophene ring interacts with the hydroxyl group of Thr77. The set of hydrogen-bond interactions for the bicyclic moiety of biotin is generally similar to that of the avidin–norbiotin complex (PDB ID: 1LDO).[18] When that complex is compared to the avidin–biotin complex (PDB ID: 1AVD), the only difference is the weak interaction of Thr77 with S1 (distance 3.75 Å).[16a]

Additionally, the tetrahydrothiophene ring of **3** is stabilized by the aromatic residues Phe79, Trp97, and Trp70 and also Trp110 from the symmetry-related monomer. In the first part of the linker chain, O2 interacts with the nitrogens of Ala39 and Thr38 from the loop L3-4, whereas N3 interacts via the hydrogen bond with OH of Ser75 (Table 3). The second part of the ligand aliphatic chain is stabilized in the protein-binding site by a close interaction of O3 with the ligand from the symmetry-related monomer. Moreover, N4 is stabilized by a water hydrogen network including two water molecules and the main chain atoms of Leu99, Ser101, and Lys111 (distance <3 Å). The keto oxygen bound to the ferrocene moiety (O4) is stabilized by van der Waals contacts with loop 3-4 from the symmetry-related molecule.

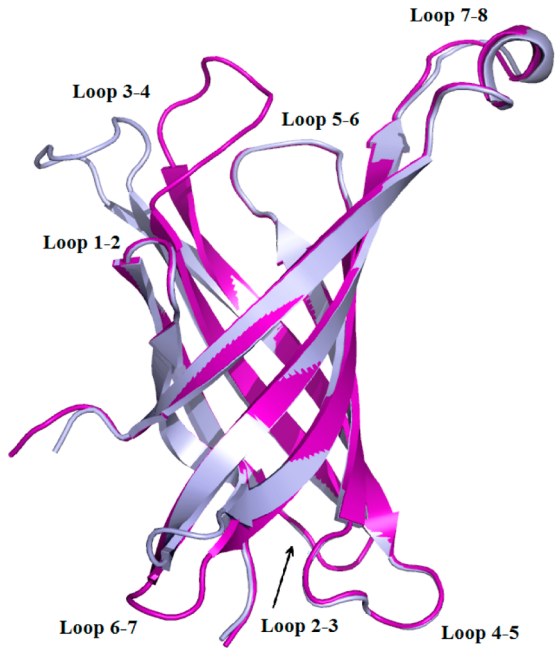

Figure 4. Structural superimposition of avidin monomers **A** (violet) and **B** (light blue) showing different conformations of loops L3-4 and L6-7.

In monomer **B** two different conformations of **3** were observed, owing to the different positioning of loop L3-4 (residues 35–45). The first conformation (I) is located parallel to the axis of the β-barrel, and the second (II) is turned into the direction of loop L3-4 and the sugar moiety attached to Asn17 (Figure 6). The bicyclic biotin moiety in both conformations interacts by hydrogen bonds with five polar residues, as presented in Table 3. The nitrogen atom in the ureido fragment (N2). similarly to the case for the avidin–homobiotin complex,[17] does not display a hydrogen-bond interaction with Thr35, as a result of a conformational change of loop L3-4. The remaining hydrogen bonds are maintained (Table 3). The tetrahydrothiophene ring is stabilized similarly as in monomer **A** through interactions with the aromatic residues. The keto oxygen (O2) from the aliphatic chain in conformation II of the ligand interacts by hydrogen bonds with Ser75 and Ser73, as in the avidin–biotin complex (PDB ID: 1AVD), and additionally by the water-mediated hydrogen bond with Ser101. The keto oxygen O2 in conformation I is stabilized only by water-mediated hydrogen interactions with Ser75 and Ser101. Most interestingly, ligand **3** in conformation II makes π-electron contacts between both the cyclopentadienyl rings of ferrocene and two residues: Ala36 from loop L3-4 of monomer **B** and Trp110 from the symmetry-related monomer. Moreover, the

dx.doi.org/10.1021/om4003126 | *Organometallics* XXXX, XXX, XXX–XXX

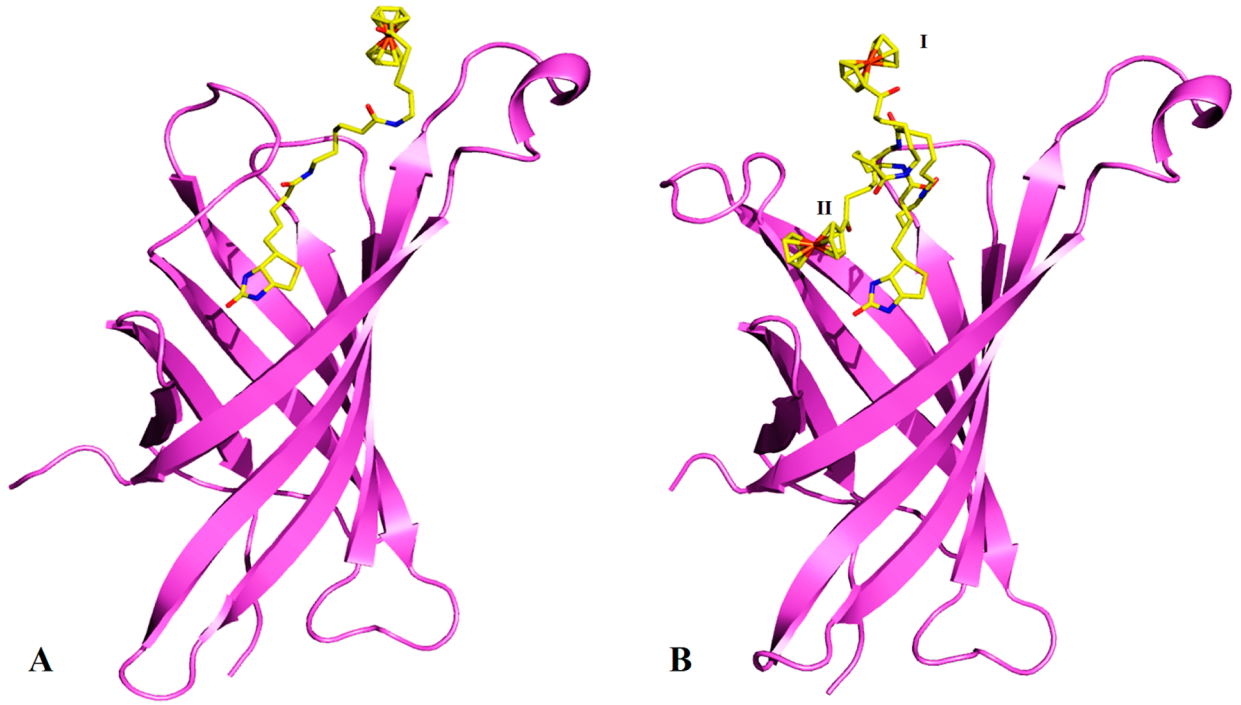

Figure 5. Ligand **3** (yellow) in the binding pocket of monomers **A** and **B** of avidin (violet). In monomer **B** two conformations of the ligand (I and II) are shown.

keto oxygen O4 of the ligand acts as an acceptor to the hydroxyl group of Thr35.

Generally, the interactions of **3** with avidin appear to be different in the two monomers. The biotin bicyclic moiety is located in the deepest part of the binding pocket in both monomers, and most interactions found for the ligand in its complex with avidin are maintained. Due to the high flexibility of the linker, the interaction of the ferrocene moiety differs in both monomers. As a result of the this flexibility and metallocene moiety interaction with the protein in monomer **B**, a spatial rearrangement of loop L3-4 takes place. In this context the crystal structure of **avidin-3** is considered to be important for a better understanding of the avidin−ligand interactions. It is also worth noting that only a few crystal structures of the complexes of proteins with ferrocene-derived ligands have hitherto been reported.[19]

CONCLUSIONS

We demonstrated the feasibility of a direct Friedel−Crafts acylation of ferrocene with biotin-derived acids featuring aminoacyl linkers and with desthiobiotin. The resulting conjugates along with compound **1** obtained by acylation of ferrocene with biotin display high affinity for avidin and cytotoxicity against SW620 cancer cell lines, thus expressing a high level of the biotin receptor. This suggests that the biotin moiety may serve as a biological vector for the targeted cancer cells with cytotoxic ferrocenyl groups. Finally, an X-ray diffraction study of **avidin-3** revealed unusual protein−ligand interactions and stabilization of different conformations of the ligand in the protein binding pocket.

EXPERIMENTAL SECTION

General Considerations. ^{1}H and ^{13}C NMR spectra were recorded on a Bruker ARX 600 MHz spectrometer (600 MHz for ^{1}H and 151 MHz for ^{13}C). Chemical shifts in the ^{1}H spectra were referenced relative to solvent signals: $CDCl_3$, δ 7.27 ppm for ^{1}H and δ 77.00 ppm for ^{13}C; CD_3OD, δ 3.31 ppm for ^{1}H and δ 49.15 ppm for ^{13}C; DMSO-d_6, δ 2.50 for ^{1}H and δ 39.51 for ^{13}C. Spectra were recorded at room temperature (291 K); chemical shifts are in ppm and coupling constants in Hz. EI and HR-EI analyses were performed in the positive mode at 75 eV. Thin-layer chromatography (TLC) was performed on aluminum sheets precoated with Merck 5735 Kieselgel 60F254. Column chromatography was carried out on silica gel 60 (0.040−0.063 mm, 230−400 mesh, Fluka). Dichloromethane was distilled from calcium hydride and stored over activated molecular sieves 4A (8−12 mesh). Reactions with ferrocene were carried out using standard Schlenk techniques. Chemicals, biochemicals, and solvents (HPLC grade) were purchased from Sigma-Aldrich or AK Scientific (USA) and used as received. Avidin from egg white was purchased from Interchim; its activity was equal to 14.8 units/mg. A 1 mg mL^{-1} stock solution of avidin was prepared in PBS and kept at 4 °C. Stock solutions of biotin (2 mg mL^{-1}), desthiobiotin (1 mg mL^{-1}), and conjugates (1 mg mL^{-1}) were prepared in PBS and DMSO, respectively.

Synthesis of Compounds. Compounds **1**[4] and 6-biotinamidohexanoic acid (**5**)[20] were prepared according to published procedures.

6-Acetamidohexanoic Acid (7). To a stirred slurry of 6-aminohexanoic acid (5.0 g, 38.1 mmol)) and sodium carbonate (8.2 g, 77.4 mmol) in anhydrous THF (50 mL) was added a solution of acetyl chloride (3.29 g, 2.98 mL, 41.9 mmol) in THF (5 mL). The resulting mixture was stirred in a water cooling bath (exothermic reaction!) until the reaction temperature decreased to room temperature. After 4 h, distilled water (50 mL) was added and the resulting solution was acidified with hydrochloric acid (up to pH 0−1). The product was extracted 5 times with ethyl acetate (100 mL each portion), the extracts were dried over sodium sulfate, and the solvent was evaporated. Yield: 1.9 g. The crude product was washed with diethyl ether and *n*-pentane and used in the next step without further purification. Its spectroscopic data were identical with those of the authentic sample.[21] ^{1}H NMR (DMSO-d_6): δ 11.95 (s, 1 H, COOH), 7.75 (br s, 1 H, NH), 2.95−3.03 (m, 2 H, H-6), 2.18 (t, J = 7.53 Hz, 2 H, H-2), 1.77 (s, 3 H, CH_3), 1.44−1.52 (m, 2 H, H-3), 1.33−1.41 (m, 2 H, H-5), 1.21−1.29 (m, 2 H, H-4). ^{13}C NMR (DMSO-d_6): δ 174.3 (CO), 168.8 (CO), 38.3, 33.6, 28.8, 26.0, 24.2, 22.6. MS (EI): (M^+) 341.0. HRMS (EI): calcd for $C_{18}H_{23}FeNO_2$ 341.10783, found

dx.doi.org/10.1021/om4003126 | *Organometallics* XXXX, XXX, XXX−XXX

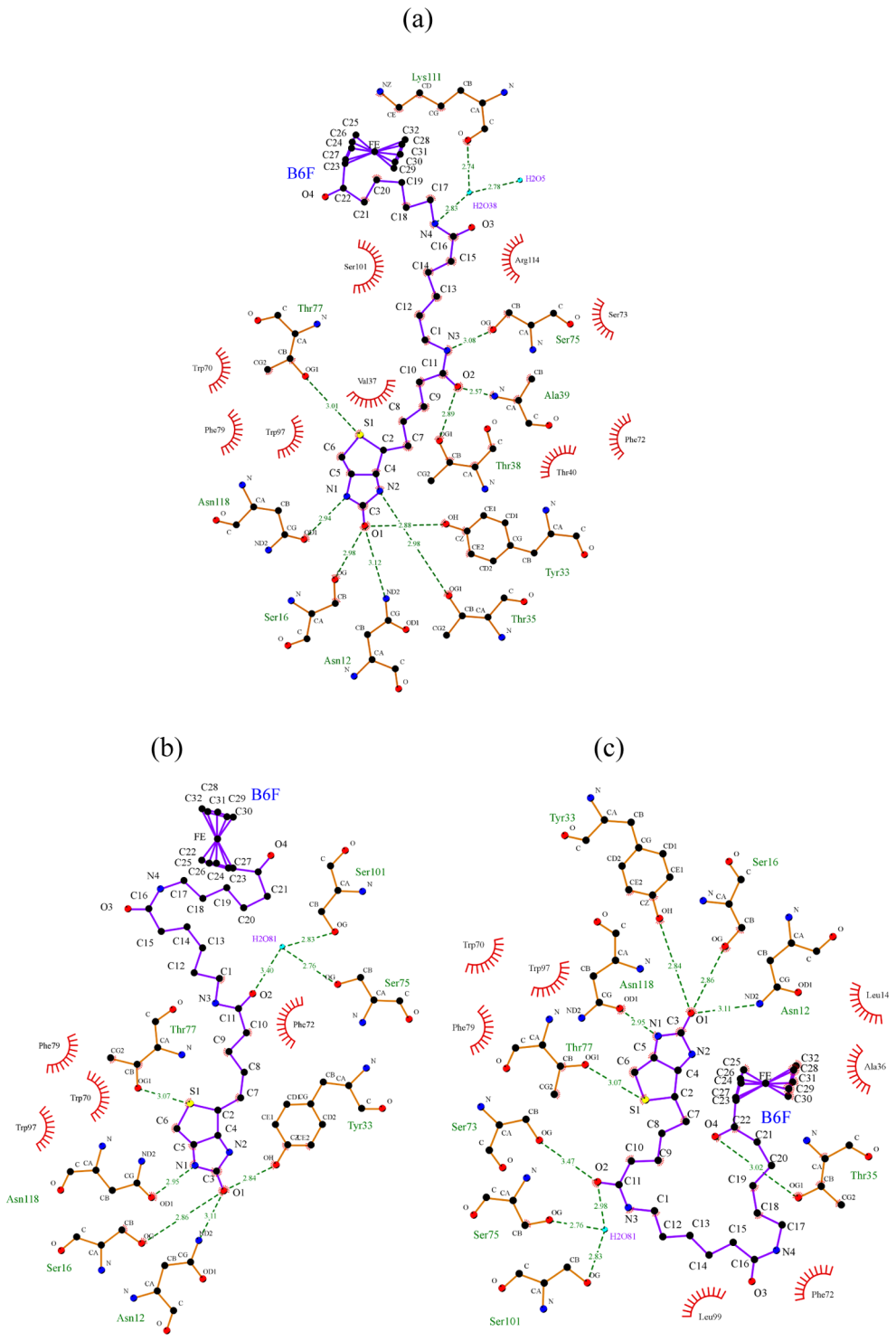

Figure 6. Protein–ligand interactions in **avidin-3**: (a) in monomer **A**; (b) in monomer **B** (ligand conformation I); (c) in monomer **B** (ligand conformation II).

341.10666 (δ 1.08641 ppm). Anal. Calcd for $C_{18}H_{23}FeNO_2$: C, 63.36; H, 6.79; N, 4.10. Found: C, 63.31; H, 6.75; N, 4.10.

*6-(6-Biotinamidohexanamido)hexanoic Acid (**6**).* To a solution of 6-biotinamidohexanoic acid (**5**; 357.5 mg, 1.0 mmol) in a mixture of DMF (10 mL) and water (2 mL) were added DIPEA (381.4 mg, 514 μL, 2.95 mmol), TSTU (380 mg, 1.26 mmol), and (after stirring at room temperature for 20 min) 6-aminohexanoic acid (196 mg, 1.5 mmol). After 1 h the solvents were evaporated to dryness, the solid residue was dissolved in 50% ethanol (10 mL), and the solution was acidified with concentrated hydrochloric acid. The resulting solution was kept at 4 °C for 20 h, and the precipitated product was filtered off, washed with water, and dried at 40 °C under vacuum (ca. 5 Pa). Yield: 198 mg. The product was used in the next step without further purification. Its spectral data were identical with those of the authentic sample.[22] ^{1}H NMR (DMSO-d_6): δ 11.94 (br s, 1 H, COOH), 7.79–7.59 (m, 2 H, 2 × NH, H-12 and H-19), 6.39 (br s, 1 H, 3-NH), 6.33 (br s, 1 H, 1-NH), 4.30 (dd, J = 5.1, 7.3 Hz, 1 H, H-6a), 4.13 (dd, J = 4.7, 7.0 Hz, 1 H, H-4a), 3.13–3.05 (m, 1 H, H-4, CH_2-alkyl chain), 3.04–2.97 (m, 4 H, CH_2-alkyl chain), 2.82 (dd, J = 5.3, 12.4 Hz, 1 H, H-6), 2.58 (d, J = 12.4 Hz, 1 H, H-6), 2.18 (t, J = 7.5 Hz, 2 H, CH_2-alkyl chain), 2.08–2.00 (m, 4 H, CH_2-alkyl chain), 1.66–1.57

dx.doi.org/10.1021/om4003126 | *Organometallics* XXXX, XXX, XXX–XXX

Table 4. Crystallographic Data and Refinement Statistics for the Complex of Avidin with 3[a] (PDB: 4JHQ)

X-ray Data Collection and Processing Statistics	
radiation source	BESSY BEAMLINE 14.2
wavelength (Å)	0.91841
temp (K)	100
rotation range (deg)	0.5
space group	$P2_12_12$
unit cell (Å)	a = 69.69, b = 78.66, c = 42.76
molecules in asymmetric unit	2
completeness (%)	96.5 (82.6)
redundancy	4.6 (3.9)
$I/\sigma(I)$	31.45 (6.30)
R_{marge}[b] (%)	4.3 (17.9)
Refinement Statistics	
resolution range high (Å)	1.99 (1.99)
resolution range low (Å)	28.96 (2.05)
R_{work}[c]/R_{free}[c] (%)	16.22/21.02
RMSD bond lengths (Å)	0.018
RMSD bond angles (deg)	1.957
av B factor (Å^2)	37.00
Ramachandran Plot	
most favored regions (%)	93.5
allowed regions (%)	6.5
generously allowed regions (%)	0.0
disallowed regions (%)	0.0

[a]Values in parentheses are for the last resolution shell. [b]$R_{merge} = \sum_h\sum_j|I_{hj} - \langle I_h\rangle|/\sum_h\sum_j I_{hj}$, where I_{hj} is the intensity of observation j of reflection h. [c]$R = \sum_h||F_o| - |F_c||/\sum_h|F_o|$ for all reflections, where F_o and F_c are observed and calculated structure factors, respectively. R_{free} is calculated analogously for the test reflections, randomly selected and excluded from the refinement.

(m, 1 H, CH_2-alkyl chain), 1.56−1.42 (m, 7 H, CH_2-alkyl chain), 1.41−1.33 (m, 4 H, CH_2-alkyl chain), 1.32−1.13 (m, 6 H, CH_2-alkyl chain). ^{13}C NMR (DMSO-d_6): δ 174.3 (CO), 171.7 (CO), 171.7 (CO), 162.6 (CO), 61.0 (C-4a), 59.2 (C-6a), 55.3 (C-4), 39.77 (C-6), 38.3, 38.2, 35.3, 35.2, 33.6, 28.9, 28.8, 28.1, 28.0, 26.1, 25.9, 25.3, 25.0, 24.2 (14 × CH_2-alkyl chain).

*6-Acetamidohexanoylferrocene (**8**).* To a suspension of **7** (174 mg, 1.0 mmol) in dichloromethane (5 mL) was added TFAA (227 mg, 150 μL, 1.08 mmol), and the mixture was stirred until the acid was completely dissolved. Then ferrocene (186 mg, 1.0 mmol) and TfOH (149 mg, 88 μL, 0.995 mmol) were added, and stirring was continued for 2 h. Quenching with water, extraction with dichloromethane, and chromatography (silica 50 mL, eluent dichloromethane−MeOH gradient 0−10% MeOH) afforded, in order of elution, acetylferrocene (11 mg, 5%, identified by comparison with an authentic sample) and **4** as an orange solid (205 mg, 60%). ^{1}H NMR ($CDCl_3$): δ 5.97 (br s, 1 H, NH), 4.75 (s, 2 H, Cp), 4.48 (d, J = 1.51 Hz, 2 H, Cp), 4.17 (s, 5 H, Cp), 3.25 (dd, J = 6.40, 5.27 Hz, 1 H, H-6), 2.69 (t, J = 7.15 Hz, 2 H, H-2), 1.96 (s, 3 H, CH_3), 1.70 (quin, J = 7.43 Hz, 2 H, H-3), 1.54 (quin, J = 7.15 Hz, 2 H, H-5), 1.33−1.42 (m, 2 H, H-4). ^{13}C NMR ($CDCl_3$): δ 204.55 (C-1), 170.62 (C-8), 79.05 (Cp-ipso), 72.22 (Cp), 69.76 (Cp), 69.30 (Cp), 39.41 (C-2 or C-6), 39.37 (C-2 or C-6), 29.39 (C-5), 26.70 (C-4), 23.96 (C-3), 23.34 (CH_3). MS (EI): (M^+) 341.0. HRMS (EI): calcd for $C_{18}H_{23}FeNO_2$ 341.10783, found 341.10666 (δ 1.08641 ppm). Anal. Calcd for $C_{18}H_{23}FeNO_2$: C, 63.36; H, 6.79; N, 4.10. Found: C, 63.31; H, 6.75; N, 4.10.

*6-Biotinamidohexanoylferrocene (**2**).* The procedure was the same as for **8**, except 6-biotinamidohexanoic acid (**5**; 177 mg, 0.495 mmol), ferrocene (94 mg, 0.505 mmol), TFAA (227 mg, 150 μL, 1.08 mmol), and TfOH (75 mg, 44 μL, 0.497 mmol) were used. Yield: 72.8 mg (28%). Orange solid. ^{1}H NMR ($CDCl_3$): δ 6.52 (br s, 1 H, 1-NH), 6.32 (t, J = 4.9 Hz, 1 H, 3-NH), 5.64 (br s, 1 H, 12-NH), 4.77 (t, J = 1.9 Hz, 2 H, Cp), 4.57−4.45 (m, 3 H, Cp and H-6a), 4.31 (d, J = 4.5 Hz, 1 H, H-4a), 4.19 (s, 5 H, Cp), 3.25 (q, J = 6.7 Hz, 2 H, H-10), 3.18−3.11 (m, 1 H, H-4), 2.90 (dd, J = 4.5, 12.8 Hz, 1 H, H-6), 2.69−2.75 (m, 3H, H-6 and H-17), 2.21 (t, J = 7.3 Hz, 2 H, CH_2-alkyl chain), 1.80−1.61 (m, 6 H, CH_2-alkyl chain), 1.56 (quin, J = 7.2 Hz, 2 H, CH_2-alkyl chain), 1.48−1.36 (m, 4 H, CH_2-alkyl chain). ^{13}C NMR ($CDCl_3$): δ 204.7 (18-CO), 173.2 (11-CO), 164.4 (2-CO), 79.0 (Cp-ipso), 72.2 (Cp), 69.8 (Cp), 69.3 (Cp), 61.8 (C-4a), 60.2 (C-6a), 55.6 (C-4), 40.5 (C-6), 39.4 (C-17), 39.2 (C-10), 36.1 (CH_2-alkyl chain), 29.4 (CH_2-alkyl chain), 28.2 (CH_2-alkyl chain), 28.1 (CH_2-alkyl chain), 26.7 (CH_2-alkyl chain), 25.8 (CH_2-alkyl chain), 24.0 (CH_2-alkyl chain). MS (EI): 525.3 (M^+). HRMS (EI): calcd for $C_{26}H_{35}FeN_3O_3S$ 525.174875 found 525.17428 (δ 1.08641 ppm). Anal. Calcd for $C_{26}H_{35}FeN_3O_3S$: C, 59.43; H, 6.71; N, 8.00. Found: C, 59.44; H, 6.93; N, 8.09.

*6-(6-Biotinamidohexanamido)hexanoylferrocene (**3**).* The procedure was the same as for **8**, except 6-(6-biotinamidohexanamido)-hexanoic acid (**6**; 94 mg, 0.200 mmol), ferrocene (37 mg, 0.200 mmol), TFAA (227 mg, 150 μL, 1.08 mmol), and TfOH (85 mg, 50 μL, 0.565 mmol) were used. Chromatography on silica (silica 25 mL, eluent dichloromethane−MeOH gradient 0−10% MeOH) and then on a SF10-8g column (Varian) afforded **8** as an orange solid. Yield: 21 mg (16.4%). ^{1}H NMR (CD_3OD): δ 4.83 (t, J = 1.88 Hz, 2 H, Cp), 4.59 (t, J = 1.88 Hz, 2 H, Cp), 4.49 (dd, J = 7.53, 4.89 Hz, 1 H, H-6a), 4.30 (dd, J = 7.91, 4.52 Hz, 1 H, H-4a), 4.23 (s, 5 H, Cp), 3.18−3.22 (m, 3 H, H-4 and CH_2-alkyl chain), 3.14−3.18 (m, 2 H, CH_2-alkyl chain), 2.92 (dd, J = 12.80, 4.89 Hz, 1 H, H-6), 2.79 (t, J = 7.34 Hz, 2 H, H-24), 2.71 (d, J = 12.80 Hz, 1 H, H-6), 2.17−2.21 (m, 4 H, CH_2-alkyl chain), 1.35−1.75 (m, 18H, CH_2-alkyl chain). ^{13}C NMR (CD_3OD): δ 208.03 (25-CO), 176.1 (11- or 18-CO), 176.1 (11- or 18-CO), 166.2 (2-CO), 80.2 (Cp-ipso), 74.0 (Cp), 71.1 (Cp), 70.8 (Cp), 63.5 (C-4a), 61.8 (C-6a), 57.1 (C-4), 41.2 (C-6), 40.6, 40.4 (2 × C), 37.2, 37.0, 30.5, 30.3, 29.9, 29.6, 27.9, 27.7, 27.1, 26.9, 25.6 (14 × CH_2-alkyl chain). MS (EI): 638.4 (M^+). HRMS (EI): calcd for $C_{32}H_{46}FeN_4O_4S$ 638.25966, found 638.25984 (δ 0.43170 ppm). Anal. Calcd for $C_{32}H_{46}FeN_4O_4S$: C, 60.18; H, 7.26; N, 8.77. Found: C, 60.05; H, 7.03; N, 8.85.

*Desthiobiotinoylferrocene (**4**).* The procedure was the same as for **8**, except D-desthiobiotin (214 mg, 1 mmol), ferrocene (187 mg, 1 mmol), TfOH (149 mg, 88 μL, 0.995 mmol), and TFAA (227 mg, 150 μL, 1.08 mmol) were used. Yield: 130 mg (34%). Orange solid. ^{1}H NMR ($CDCl_3$): δ 5.15 (br s, 1 H, 1-NH), 4.84 (br s, 1 H, 3-NH), 4.78 (t, J = 1.9 Hz, 2 H, Cp), 4.54−4.45 (m, 2 H, Cp), 4.19 (s, 5 H, Cp), 3.84 (quin, J = 6.7 Hz, 1 H, H-5), 3.75−3.67 (m, 1 H, H-4), 2.71 (t, J = 7.3 Hz, 2 H, H-11), 1.72 (quin, J = 7.2 Hz, 2 H, H-10), 1.59−1.38 (m, 5 H, CH_2-alkyl chain), 1.35−1.28 (m, 1 H, CH_2-alkyl chain), 1.13 (d, J = 6.4 Hz, 3 H, H-6). ^{13}C NMR ($CDCl_3$): δ 204.3 (12-CO), 163.5 (2-CO), 79.1 (Cp-ipso), 72.1 (Cp), 69.7 (Cp), 69.3 (Cp), 56.0 (C-4), 51.4 (C-5), 39.4 (C-11), 29.5 (CH_2-alkyl chain), 29.4 (CH_2-alkyl chain), 26.4 (CH_2-alkyl chain), 24.3 (C-10), 15.7 (C-6). MS (EI): (M^+) 382.1. HRMS (EI): calcd for $C_{20}H_{26}FeN_2O_2$ 382.13440, found 382.13399 (δ 0.97867 ppm). Anal. Calcd for $C_{20}H_{26}FeN_2O_2$: C, 62.84; H, 6.86; N, 7.33 Found: C, 62.81; H, 6.83; N, 7.28.

Competitive Binding Assay for Biotin and Desthiobiotin Conjugates. Flat-bottomed polystyrene 96-well microtiter plates (Greiner) were treated with a solution of avidin (10 μg mL^{-1}, 100 μL well^{-1}) in 0.1 M carbonate buffer pH 9.5 overnight at 4 °C. The plates were blocked by the addition of PBS containing 1% BSA (w/v) (100 μg well^{-1}) for 30 min at room temperature and washed three times with PBS containing 0.05% Tween 20 (v/v) (PBS-T, 100 μL well^{-1}). Standard solutions of biotin (0−200 nM), desthiobiotin (0−2400 nM), **2** and **3** (0−2000 nM), and **4** (0−5200 nM) were applied to a series of Micronic tubes (200 μL tube^{-1}), and HRP-biotin solution (400 ng mL^{-1}, 200 μL tube^{-1}) was added to each tube. A 100 μL amount of each solution was added in duplicate to the plates, which were incubated 30 min at room temperature. The plates were washed four times with PBS-T, and an OPD solution in citrate−phosphate buffer pH 5 and 0.16% H_2O_2 v/v (0.7 mg mL^{-1}, 100 μL well^{-1}) was added to the wells. After sufficient color development, the enzymatic reaction was stopped by H_2SO_4 (2.5 M, 50 μL well^{-1}) and the optical densities at 485 and 410 nm were read with a microliter plate reader (BMG Labtech). Data sets were fitted by nonlinear regression analysis applying the four-parameter logistic equation (1), where a and d are the upper and lower

dx.doi.org/10.1021/om4003126 | Organometallics XXXX, XXX, XXX−XXX

$$OD_{485nm} = d + \frac{a - d}{1 + ([ligand]/c)^b} \quad (1)$$

asymptotes, respectively, c is the value of the [ligand] at the inflection point (IC_{50}), and b is related to the slope at the center of the sigmoid.

The relative binding affinity (RBA) is given by eq 2.

$$RBA = \frac{IC_{50}(biotin)}{IC_{50}(ligand)} \times 100 \quad (2)$$

Determination of IC_{50} for Compounds 1−4 and 8. Cell line sensitivity to compounds **1**−**4** and **8** was determined by the modified MTT-reduction assay.[23] Cells suspended in 100 μL of medium were seeded on the 96-well plates at a density of 10000/well. The cells were allowed to attach for 24 h, and then the tested compound at the desired concentration was administered. Stock solutions of compounds **2**−**4** were prepared in DMSO, and care was taken to keep the solvent concentration identical in all wells, including controls. The final DMSO concentration did not exceed 0.01% v/v and was proven to be nontoxic to the cells. After 70 h of incubation, MTT was added to the medium to a final concentration of 1.1 mM. After a further 2 h the medium was removed and the formazane crystals were dissolved in 100 μL of DMSO. Absorbance was measured at 580 nm analytical wavelength and 720 nm reference wavelength. The results were turned into a percentage of controls, and the IC_{50} values for each cell line and substance were calculated by GraphPad Prism 4.03 software (GraphPad Inc.), using the formula

$$Y = \text{Bottom} + \frac{(\text{Top} - \text{Bottom})}{1 + 10^{(\log IC_{50} - X)\cdot(\text{HillSlope})}}$$

where Bottom is the Y value bottom plateau, Top is the Y value, HillSlope determines the steepness of the curve, and IC_{50} is the inhibitory concentration.[24]

Cell Lines. The cell lines, i.e. SW620 (human colon adenocarcinoma), COLO 205 (human colon adenocarcinoma), and HCT 116 (human colon carcinoma), were purchased from the American Tissue and Cell Collection (ATCC) and were routinely tested every 3 months for *Mycoplasma* contamination. The cells were grown respectively on high-glucose DMEM or RMPI1640 medium with the addition of Glutamax-I (Gibco brand, Invitrogen Inc.) supplemented with 10% fetal bovine serum (Invitrogen Inc.). The cells were cultured under standard cell culture conditions (37 °C, 5% CO_2, 100% relative humidity).

X-ray Structure Determination of the Complex of Avidin with Compound 3. *Crystallization.* Crystals of the complex were obtained by the hanging-drop vapor-diffusion technique. Drops were obtained by mixing avidin at a 10 mg/mL concentration with 25 mM of **3** in 15% methanol in the molar ratio 1:2, followed by 12 h of incubation. The crystals were grown at 19 °C in a drop consisting of 1 μL of protein−ligand solution and 0.5 μL of the reservoir mixture, which contained 28% polyethylene glycol monomethyl ether 5K, 0.2 M magnesium formate, and 0.1 M Bis-Tris pH 6.5.

X-ray Data Collection, Processing, Structure Determination, and Refinement. Crystals were transferred into a cryoprotectant solution consisting of the mother liquor and 50% PEG400 in a ratio of 1:1. X-ray diffraction data were collected on the 14.2 beamline at the BESSY synchrotron in Berlin, Germany to a resolution of 2.0 Å. The total number of collected images with 0.5° oscillation was 240. The crystals were orthorhombic, space group $P2_12_12$, with two protein molecules in the asymmetric unit (Figure 1). All diffraction images were processed and scaled using the HKL-2000 package.[25] The structure was phased by molecular replacement in Phaser[26] using avidin (PDB: 1VYO) as a search model and refined in REFMAC5[27] from the CCP4 package. The Coot[28] program was used for manual modeling in electron-density maps. Owing to an absence of electron density, disordered regions corresponding to residue 1 in monomers A and B, residues 126−128 in A, and residues 125−128 in B were not included in the final model. The ligand library was prepared in JLigand[29] from the CCP4 package. Data collection and processing statistics for all experiments are shown in Table 4. The ligand−protein interactions were analyzed by LIGPLOT v.4.5.3.[30]

■ ASSOCIATED CONTENT

Supporting Information

Figures giving ^{1}H NMR, MS, and HRMS spectra of compounds **2**−**8** and viability of various tumor cell lines in the presence of biotin−ferrocenyl conjugates of **2**−**4** and **8**. This material is available free of charge via the Internet at http://pubs.acs.org.

■ AUTHOR INFORMATION

Corresponding Author

*J.Z.: e-mail, janzak@uni.lodz.pl; tel, (4842) 635 58 50.

Notes

The authors declare no competing financial interest.

■ ACKNOWLEDGMENTS

We are grateful to the Polish National Science Center for financial support (Grant No.1856/B/H03/2011/40). The Polish National Science Center had no impact on the study design, on the collection, analysis and interpretation of data, on the writing of the report, and on the decision to submit this article for publication.

■ REFERENCES

(1) (a) Ornelas, C. Application of ferrocene and its derivatives in cancer research. *New J. Chem.* **2011**, *35* (10), 1973. (b) Fouda, M. F. R.; Abd-Elzaher, M. M.; Abdelsamaia, R. A.; Labib, A. A. On the medicinal chemistry of ferrocene. *Appl. Organomet. Chem.* **2007**, *21* (8), 613−625. (c) Plażuk, D.; Rychlik, B.; Błauż, A.; Domagała, S. Synthesis, electrochemistry and anticancer activity of novel ferrocenyl phenols prepared via azide-alkyne 1,3-cycloaddition reaction. *J. Organomet. Chem.* **2012**, *715* (0), 102−112. (d) Plazuk, D.; Wieczorek, A.; Blauz, A.; Rychlik, B. Synthesis and biological activities of ferrocenyl derivatives of paclitaxel. *MedChemComm* **2012**, *3* (4), 498−501.

(2) (a) Vessières, A. Metal carbonyl tracers and the ferrocifen family: Two facets of bioorganometallic chemistry. *J. Organomet. Chem.* **2013**, *734* (0), 3−16. (b) Gormen, M.; Plazuk, D.; Pigeon, P.; Hillard, E. A.; Plamont, M. A.; Top, S.; Vessières, A.; Jaouen, G. Comparative toxicity of [3]ferrocenophane and ferrocene moieties on breast cancer cells. *Tetrahedron Lett.* **2010**, *51* (1), 118−120. (c) Plazuk, D.; Vessières, A.; Hillard, E. A.; Buriez, O.; Labbé, E.; Pigeon, P.; Plamont, M. A.; Amatore, C.; Zakrzewski, J.; Jaouen, G. A [3]ferrocenophane polyphenol showing a remarkable antiproliferative activity on breast and prostate cancer cell lines. *J. Med. Chem.* **2009**, *52* (15), 4964−4967.

(3) (a) Navarro, M.; Castro, W.; Biot, C. Bioorganometallic Compounds with Antimalarial Targets: Inhibiting Hemozoin Formation. *Organometallics* **2012**, *31* (16), 5715−5727. (b) Chavain, N.; Biot, C. Organometallic complexes: new tools for chemotherapy. *Curr. Med. Chem.* **2010**, *17* (25), 2729−2745. (c) Dive, D.; Biot, C. Ferrocene Conjugates of Chloroquine and other Antimalarials: the Development of Ferroquine, a New Antimalarial. *ChemMedChem* **2008**, *3* (3), 383−391. (d) Dubar, F.; Khalife, J.; Brocard, J.; Dive, D.; Biot, C. Ferroquine, an Ingenious Antimalarial Drug −Thoughts on the Mechanism of Action. *Molecules* **2008**, *13* (11), 2900−2907.

(4) Plazuk, D.; Zakrzewski, J.; Salmain, M. Biotin as acylating agent in the Friedel-Crafts reaction. Avidin affinity of biotinyl derivatives of ferrocene, ruthenocene and pyrene and fluorescence properties of 1-biotinylpyrene. *Org. Biomol. Chem.* **2011**, *9* (2), 408−417.

(5) (a) Bildstein, L.; Dubernet, C.; Couvreur, P. Prodrug-based intracellular delivery of anticancer agents. *Adv. Drug Delivery Rev.* **2011**, *63* (1−2), 3−23. (b) Yang, W.; Cheng, Y.; Xu, T.; Wang, X.; Wen, L.-p. Targeting cancer cells with biotin−dendrimer conjugates.

Eur. J. Med. Chem. **2009**, *44* (2), 862−868. (c) Russell-Jones, G.; McTavish, K.; McEwan, J.; Rice, J.; Nowotnik, D. Vitamin-mediated targeting as a potential mechanism to increase drug uptake by tumours. *J. Inorg. Biochem.* **2004**, *98* (10), 1625−1633.

(6) (a) Ojima, I. Guided Molecular Missiles for Tumor-Targeting Chemotherapy—Case Studies Using the Second-Generation Taxoids as Warheads. *Acc. Chem. Res.* **2007**, *41* (1), 108−119. (b) Chen, S.; Zhao, X.; Chen, J.; Chen, J.; Kuznetsova, L.; Wong, S. S.; Ojima, I. Mechanism-Based Tumor-Targeting Drug Delivery System. Validation of Efficient Vitamin Receptor-Mediated Endocytosis and Drug Release. *Bioconjugate Chem.* **2010**, *21* (5), 979−987.

(7) Hirsch, J. D.; Eslamizar, L.; Filanoski, B. J.; Malekzadeh, N.; Haugland, R. P.; Beechem, J. M.; Haugland, R. P. Easily reversible desthiobiotin binding to streptavidin, avidin, and other biotin-binding proteins: uses for protein labeling, detection, and isolation. *Anal. Biochem.* **2002**, *308* (2), 343−357.

(8) Muto, Y.; Murai, Y.; Sakihama, Y.; Hashidoko, Y.; Hashimoto, M. Effective Friedel-Crafts Acylation of Biotin Acid Chloride in Trifluoromethanesulfonic Acid. *Biosci., Biotechnol., Biochem.* **2012**, *76* (11), 2162−2164.

(9) Zempleni, J.; Wijeratne, S. S. K.; Hassan, Y. I. *Biotin. BioFactors* **2009**, *35* (1), 36−46.

(10) Plazuk, D.; Zakrzewski, J. Friedel-Crafts acylation of ferrocene with alkynoic acids. *J. Organomet. Chem.* **2009**, *694* (12), 1802−1806.

(11) Anderson, K. W.; Tepe, J. J. The First Intermolecular Friedel−Crafts Acylation with β-Lactams. *Org. Lett.* **2002**, *4* (3), 459−461.

(12) (a) Katritzky, A. R.; Jiang, R.; Suzuki, K. N-Tfa- and N-Fmoc-(α-aminoacyl)benzotriazoles as Chiral C-Acylating Reagents under Friedel−Crafts Reaction Conditions. *J. Org. Chem.* **2005**, *70* (13), 4993−5000. (b) Di Gioia, M. L.; Leggio, A.; Liguori, A.; Napoli, A.; Siciliano, C.; Sindona, G. Facile Approach to Enantiomerically Pure α-Amino Ketones by Friedel−Crafts Aminoacylation and Their Conversion into Peptidyl Ketones. *J. Org. Chem.* **2001**, *66* (21), 7002−7007. (c) Itoh, O.; Honnami, T.; Amano, A.; Murata, K.; Koichi, Y.; Sugita, T. Friedel-Crafts .alpha.-aminoacylation of alkylbenzene with a chiral N-carboxy-.alpha.-amino acid anhydride without loss of chirality. *J. Org. Chem.* **1992**, *57* (26), 7334−7338. (d) Nordlander, J. E.; Njoroge, F. G.; Payne, M. J.; Warman, D. N-(Trifluoroacetyl)-.alpha.-amino acid chlorides as chiral reagents for Friedel-Crafts synthesis. *J. Org. Chem.* **1985**, *50* (19), 3481−3484. (e) Nordlander, J. E.; Payne, M. J.; Njoroge, F. G.; Balk, M. A.; Laikos, G. D.; Vishwanath, V. M. Friedel-Crafts acylation with N-(trifluoroacetyl)-.alpha.-amino acid chlorides. Application to the preparation of .beta.-arylalkylamines and 3-substituted 1,2,3,4-tetrahydroisoquinolines. *J. Org. Chem.* **1984**, *49* (22), 4107−4111. (f) Buckley, T. F.; Rapoport, H. alpha.-Amino acids as chiral educts for asymmetric products. Amino acylation with N-acylamino acids. *J. Am. Chem. Soc.* **1981**, *103* (20), 6157−6163.

(13) (a) Raja, E. K.; DeSchepper, D. J.; Nilsson Lill, S. O.; Klumpp, D. A. Friedel−Crafts Acylation with Amides. *J. Org. Chem.* **2012**, *77* (13), 5788−5793. (b) Raja, E. K.; Nilsson Lill, S. O.; Klumpp, D. A. Friedel-Crafts-type reactions with ureas and thioureas. *Chem. Commun.* **2012**, *48* (65), 8141−8143.

(14) (a) McMahon, R. J., *Avidin-Biotin Interactions: Methods and Applications*; Humana Press: New York, 2008. (b) Hermanson, G. T. In *Bioconjugate Techniques*, 2nd ed.; Academic Press: New York, 2008; Chapter 23 (Avidin−Biotin Systems), pp 900−923. (c) Aslam, M.; Dent, A., *Bioconjugation: protein coupling techniques for the biomedical sciences*; Macmillan Reference: 1998. (d) Wilchek, M.; Bayer, E. A.; Livnah, O. Essentials of biorecognition: The (strept)avidin−biotin system as a model for protein−protein and protein−ligand interaction. *Immunol. Lett.* **2006**, *103* (1), 27−32. (e) Stayton, P. S.; Freitag, S.; Klumb, L. A.; Chilkoti, A.; Chu, V.; Penzotti, J. E.; To, R.; Hyre, D.; Le Trong, I.; Lybrand, T. P.; Stenkamp, R. E. Streptavidin−biotin binding energetics. *Biomol. Eng.* **1999**, *16* (1−4), 39−44. (f) Pordea, A.; Ward, T. R. Artificial Metalloenzymes: Combining the Best Features of Homogeneous and Enzymatic Catalysis. *Synlett* **2009**, *2009* (20), 3225−3236. (g) Steinreiber, J.; Ward, T., Artificial Metalloenzymes for Enantioselective Catalysis Based on the Biotin−Avidin Technology. In *Bio-inspired Catalysts*; Ward, T., Ed.; Springer: Berlin, Heidelberg, 2009; Vol. *25*, pp 93−112. (h) Thomas, C. M.; Ward, T. R. Design of artificial metalloenzymes. *Appl. Organomet. Chem.* **2005**, *19* (1), 35−39. (i) Kasuya, T.; Jung, J.; Kinoshita, R.; Goh, Y.; Matsuzaki, T.; Iijima, M.; Yoshimoto, N.; Tanizawa, K.; Kuroda, S. i., Chapter 8 - Bio-Nanocapsule−Liposome Conjugates for In Vivo Pinpoint Drug and Gene Delivery. In *Methods in Enzymology*; Nejat, D., Ed.; Academic Press: New York, 2009; Vol. *464*, pp 147−166. (j) Dancey, G.; Begent, R.; Meyer, T. Imaging in targeted delivery of therapy to cancer. *Targ. Oncol.* **2009**, *4* (3), 201−217. (k) Huang, S.-L. Liposomes in ultrasonic drug and gene delivery. *Adv. Drug Delivery Rev.* **2008**, *60* (10), 1167−1176. (l) Niemeyer, C. M. Nanoparticles, Proteins, and Nucleic Acids: Biotechnology Meets Materials Science. *Angew. Chem., Int. Ed.* **2001**, *40* (22), 4128−4158. (m) Katz, E.; Willner, I. Integrated Nanoparticle−Biomolecule Hybrid Systems: Synthesis, Properties, and Applications. *Angew. Chem., Int. Ed.* **2004**, *43* (45), 6042−6108.

(15) (a) Ulrich, N. C.; Kuder, C. H.; Hohl, R. J.; Wiemer, D. F. Biologically active biotin derivatives of schweinfurthin F. *Bioorg. Med. Chem. Lett.* **2010**, *20* (22), 6716−6720. (b) Kita, M.; Hirayama, Y.; Sugiyama, M.; Kigoshi, H. Development of Highly Cytotoxic and Actin-Depolymerizing Biotin Derivatives of Aplyronine A. *Angew. Chem., Int. Ed.* **2011**, *50* (42), 9871−9874. (c) Zhong, B.; Lama, R.; Smith, K. M.; Xu, Y.; Su, B. Design and synthesis of a biotinylated probe of COX-2 inhibitor nimesulide analog JCC76. *Bioorg. Med. Chem. Lett.* **2011**, *21* (18), 5324−5327. (d) Kang, Y.; Lou, C.; Ahmed, K. B. R.; Huang, P.; Jin, Z. Synthesis of biotinylated OSW-1. *Bioorg. Med. Chem. Lett.* **2009**, *19* (17), 5166−5168.

(16) (a) Pugliese, L.; Coda, A.; Malcovati, M.; Bolognesi, M. Three-dimensional Structure of the Tetragonal Crystal Form of Egg-white Avidin in its functional Complex with Biotin at 2·7 Å Resolution. *J. Mol. Biol.* **1993**, *231* (3), 698−710. (b) Livnah, O.; Bayer, E. A.; Wilchek, M.; Sussman, J. L. Three-dimensional structures of avidin and the avidin-biotin complex. *Proc. Natl. Acad. Sci. U.S.A.* **1993**, *90* (11), 5076−5080.

(17) Chou, K.-C.; Carlacci, L.; Maggiora, G. G. Conformational and geometrical properties of idealized β-barrels in proteins. *J. Mol. Biol.* **1990**, *213* (2), 315−326.

(18) Pazy, Y.; Kulik, T.; Bayer, E. A.; Wilchek, M.; Livnah, O. Ligand Exchange between Proteins: Exchange of biotin and biotin derivatives between avidin and streptavidin. *J. Biol. Chem.* **2002**, *277* (34), 30892−30900.

(19) (a) Salmon, A. J.; Williams, M. L.; Hofmann, A.; Poulsen, S.-A. Protein crystal structures with ferrocene and ruthenocene-based enzyme inhibitors. *Chem. Commun.* **2012**, *48* (17), 2328−2330. (b) Heine, A.; Stura, E. A.; Yli-Kauhaluoma, J. T.; Gao, C.; Deng, Q.; Beno, B. R.; Houk, K. N.; Janda, K. D.; Wilson, I. A. An Antibody exo Diels-Alderase Inhibitor Complex at 1.95 Angstrom Resolution. *Science* **1998**, *279* (5358), 1934−1940.

(20) Skander, M.; Humbert, N.; Collot, J.; Gradinaru, J.; Klein, G.; Loosli, A.; Sauser, J.; Zocchi, A.; Gilardoni, F.; Ward, T. R. Artificial Metalloenzymes: (Strept)avidin as Host for Enantioselective Hydrogenation by Achiral Biotinylated Rhodium−Diphosphine Complexes. *J. Am. Chem. Soc.* **2004**, *126* (44), 14411−14418.

(21) Kvarda, J.; Prokopová, I.; Kondelík, P. Reactivity of 6-Hexanelactam Cyclic Oligomers, 1. Acidolysis. *Macromol. Chem. Phys.* **2001**, *202* (1), 133−138.

(22) Yamazaki, Y.; Kohno, K.; Yasui, H.; Kiso, Y.; Akamatsu, M.; Nicholson, B.; Deyanat-Yazdi, G.; Neuteboom, S.; Potts, B.; Lloyd, G. K.; Hayashi, Y. Tubulin Photoaffinity Labeling with Biotin-Tagged Derivatives of Potent Diketopiperazine Antimicrotubule Agents. *ChemBioChem* **2008**, *9* (18), 3074−3081.

(23) Carmichael, J.; DeGraff, W. G.; Gazdar, A. F.; Minna, J. D.; Mitchell, J. B. Evaluation of a Tetrazolium-based Semiautomated Colorimetric Assay: Assessment of Chemosensitivity Testing. *Cancer Res.* **1987**, *47* (4), 936−942.

(24) Giraldo, J.; Vivas, N. M.; Vila, E.; Badia, A. Assessing the (a)symmetry ofconcentration-effect curves: empirical versus mechanistic models. *Pharmacol. Ther.* **2002**, *95*, 21−45.

(25) Otwinowski, Z.; Minor, W., [20] Processing of X-ray diffraction data collected in oscillation mode. In *Methods in Enzymology*; Carter, C. W., Jr., Ed. Academic Press: New York, 1997; Vol. *276*, pp 307−326.
(26) (a) McCoy, A. J. Solving structures of protein complexes by molecular replacement with Phaser. *Acta Crystallographica Section D* **2007**, *63* (1), 32−41. (b) McCoy, A. J.; Grosse-Kunstleve, R. W.; Adams, P. D.; Winn, M. D.; Storoni, L. C.; Read, R. J. Phaser crystallographic software. *J. Appl. Crystallogr.* **2007**, *40* (4), 658−674.
(27) Murshudov, G. N.; Vagin, A. A.; Dodson, E. J. Refinement of Macromolecular Structures by the Maximum-Likelihood Method. *Acta Crystallographica Section D* **1997**, *53* (3), 240−255.
(28) Emsley, P.; Cowtan, K. Coot: model-building tools for molecular graphics. *Acta Crystallogr., Sect. D* **2004**, *60* (12), 2126−2132.
(29) Lebedev, A. A.; Young, P.; Isupov, M. N.; Moroz, O. V.; Vagin, A. A.; Murshudov, G. N. JLigand: a graphical tool for the CCP4 template-restraint library. *Acta Crystallogr., Sect. D* **2012**, *68* (4), 431−440.
(30) Wallace, A. C.; Laskowski, R. A.; Thornton, J. M. LIGPLOT: a program to generate schematic diagrams of protein-ligand interactions. *Protein Eng.* **1995**, *8* (2), 127−34.